RSC Advances

PAPER

View Article Online
View Journal | View Issue



Cite this: *RSC Adv.*, 2023, **13**, 25717

# Novel flurbiprofen clubbed oxadiazole derivatives as potential urease inhibitors and their molecular docking study†

Sajjad Ahmad,[a] Momin Khan,[a]* Aftab Alam,[b] Amar Ajmal,[c] Abdul Wadood,[c] Azim Khan,[d] Abdullah F. AlAsmari,[e] Metab Alharbi,[e] Abdulrahman Alshammari[e] and Abdul Shakoor[a]

In this study, twenty eight novel oxadiazole derivatives (**5–32**) of the marketed available non-steroidal anti-inflammatory drug (NSAID), (*S*)-flurbiprofen (**1**), were synthesized *via* $I_2$ mediated cyclo-addition reaction in better yields. The synthesized hydrazone-Schiff bases were cyclized with iodine by using potassium hydroxide as a base in DMSO solvent to obtain oxadiazole derivatives (**5–32**). Structures of the synthesized products were confirmed with HR-ESI-MS, $^1$H-NMR spectroscopy and CHN analysis. After structure confirmations all analogs were evaluated for urease (*in vitro*) inhibitory activity. Amongst the series, fourteen compounds **20**, **26**, **30**, **24**, **21**, **16**, **28**, **31**, **32**, **7**, **19**, **13**, **10**, and **6** were found to be excellent inhibitors of urease enzyme, having $IC_{50}$ values of 12 ± 0.9 to 20 ± 0.5 μM, better than the standard thiourea ($IC_{50}$ = 22 ± 2.2 μM), whereas the remaining fourteen derivatives displayed good to moderate activity. The *in silico* study was executed to analyse the interaction between the active site of the enzyme (urease) and the produced compounds. The docking study revealed that compounds **20**, **26**, **30**, **24**, **21**, **16**, **28**, **31**, **32**, **7**, **19**, **13**, **10**, and **6** had lower docking scores than the standard compound thiourea and revealed better interactions with the urease enzyme.

Received 8th June 2023
Accepted 16th August 2023

DOI: 10.1039/d3ra03841f

rsc.li/rsc-advances



## 1. Introduction

Heterocyclic compounds, often known as heterocycles, are organic compounds that have at least one or more atoms in the ring other than carbon.[1] These substances have wide-ranging biotic and pharmacological applications.[2] Among heterocyclic compounds, 1,3,4-oxadiazole has emerged as an important framework for the synthesis of novel pharmaceuticals.[3] Anti-hypertensive, anti-convulsant, anti-diabetic, anti-oxidant, anti-cancer, analgesic, anti-inflammatory, anti-bacterial, and anti-fungal qualities are only a few of the biological uses of compounds containing the 1,3,4-oxadiazole moiety.[4–6] Because of its precious structure, which has significant biological potential, 1,3,4-oxadiazole containing heterocycles are crucial for molecular planning.[7] These compounds can undergo a variety of processes. A number of medicinal molecules of the oxadiazole scaffold are utilized as medications in the market, including the well-known anti-hypertensive nesapidil, the strong PDF inhibitor furamizole, the HIV integrase inhibitor raltegravir, and the anti-cancer agent zibotentan.[8,9] In addition, a number of oxadiazoles have been discovered to exhibit strong monoamine oxidase inhibitory potential and to be efficacious against lipoxygenase at the nano molar level.[10]

Non-steroidal anti-inflammatory drugs (NSAIDs) are important approved medications used throughout the world for the management of fever, pain, and inflammation because of their analgesic, anti-inflammatory and anti-pyretic properties.[11] Flurbiprofen is a familiar NSAID identified by the trade term ANSAID and was sold for the first time by Pfizer in 1977 in Europe.[12] This medication is well-known for its anti-inflammatory properties because it works by inhibiting the cyclooxygenase enzymes COX-I and COX-II, which block the production of prostaglandins.[13] Flurbiprofen, a significant member of the NSAID group, is frequently utilized to diminish migraines, inflammation, osteoarthritis, acute gout, post-operative inflammation, soft tissue injuries, herpetic stromal keratitis, rheumatoid arthritis, and periodontal surgery.[14–16]

The primary objective of the current research study is to facilitate the transformation of a number of medications that are currently on the market into diverse molecules. Subsequently, these manufactured derivatives will be tested for

[a]*Department of Chemistry, Abdul Wali Khan University, Mardan-23200, Pakistan. E-mail: mominkhan@awkum.edu.pk*
[b]*Department of Chemistry, University of Malakand, Chakdara, Lower Dir 18800, Pakistan*
[c]*Department of Biochemistry, Abdul Wali Khan University, Mardan-23200, Pakistan*
[d]*Laboratory for Corrosion and Protection, Institute of Metal Research, Chinese Academy of Sciences, Shenyang, 62 Wencui Road, 110016, China*
[e]*Department of Pharmacology and Toxicology, College of Pharmacy, King Saud University, Riyadh 11451, Saudi Arabia*

† Electronic supplementary information (ESI) available. See DOI: https://doi.org/10.1039/d3ra03841f

a range of biological functions. In the past, a number of drug compounds were created and tested for their biological effects, and they were found to have strong enzyme inhibitory properties. For instance, compounds prepared from metronidazole exhibited outstanding α-glucuronidase and α-amylase inhibitory action, while derivatives of piroxicam were successfully tested for their anti-nociceptive activity. Similar to that, NSAIDs are also assessed for their actions that inhibit enzymes, which produce good to moderate results.[17,18] Inhibitors of the SGLT2, α-amylase and α-glucosidase enzymes that include biphenyl rings have recently been identified as possible pointers for the cure of type-2 diabetes mellitus.[19–22] Similarly Alam *et al.* reported the synthesis of flurbiprofen hydrazone derivatives as potent α-glucosidase inhibitors.[11] However, Khan *et al.* reported the synthesis of 2-mercaptooxadiazole derivatives of flurbiprofen as excellent α-amylase inhibitors.[6] Additionally, Taha *et al.* discovered that a variety of analogues containing fluorine atoms attached to the benzene rings had strong α-glucosidase inhibitory action and mentioned that the fluorine group is responsible for the potency of the active compounds (Fig. 1).[23] The main scaffold of the flurbiprofen nucleus is fluoro substituted biphenyl rings. We, therefore, considered investigating the urease inhibitory potential of flurbiprofen derivatives.

## 2. Results and discussion

### 2.1. Chemistry

Twenty eight oxadiazole derivatives (**5–32**) based on the (*S*)-flurbiprofen nucleus were successfully synthesized and purified through multi-step reactions as part of on-going efforts to find biologically/pharmacologically active and powerful urease inhibitors. Prior to being refluxed with excess hydrazine hydrate in ethanol to produce the desired hydrazide of flurbiprofen in noble to brilliant yields, commercially available flurbiprofen acid was first heated on continual stirring with sulfuric acid in absolute ethanol to acquire ester. To create the hydrazone Schiff base derivatives of flurbiprofen, the hydrazide was further refluxed with various substituted aromatic aldehydes in the presence of a catalytic amount of acetic acid in ethanol. Finally using iodine, potassium hydroxide and DMSO as a solvent the hydrazone Schiff bases were cyclized to oxadiazole (Scheme 1).[24] After the reaction was completed, unreacted iodine was removed using 5% sodium thiosulphate ($Na_2S_2O_3$). HR-ESI-MS and $^1$H-NMR spectroscopy were used to confirm the structures of the synthesized oxadiazole derivatives and finally, these products were analysed for urease (*in vitro*) inhibitory activity.

### 2.2. *In vitro* urease inhibitory activity

The synthesized products were evaluated for their *in vitro* urease inhibitory potential and compared to the standard thiourea ($IC_{50}$ = 22 ± 2.2 μM). Among the synthesized series, fourteen compounds **20**, **26**, **30**, **24**, **21**, **16**, **28**, **31**, **32**, **7**, **19**, **13**, **10**, and **6** were found to be the most potent urease inhibitors better than the standard, having $IC_{50}$ values of 12 ± 0.9, 12 ± 0.1, 12 ± 0.1, 13 ± 0.1, 13 ± 0.2, 13 ± 0.2, 14 ± 0.3, 15 ± 0.3, 15 ± 0.3, 16 ± 0.1, 16 ± 0.3, 16 ± 0.9, 20 ± 0.5, and 20 ± 0.5 μM, respectively. Furthermore, compounds **15** ($IC_{50}$ = 31 ± 1.2 μM), **22** ($IC_{50}$ = 31 ± 1.4 μM), **27** ($IC_{50}$ = 34 ± 2.4 μM), **14** ($IC_{50}$ = 35 ± 1.2 μM), **25** ($IC_{50}$ = 35 ± 1.5 μM), **17** ($IC_{50}$ = 36 ± 1.2 μM), **23** ($IC_{50}$ = 37 ± 1.4 μM), **18** ($IC_{50}$ = 38 ± 1.4 μM), and **5** ($IC_{50}$ = 39 ± 1.2 μM) exhibited significant urease inhibitory activity, while five compounds **8**, **11**, **29**, **9** and **12** showed moderate to less activity in the range of 41 ± 1.2 to 74 ± 1.3 μM (Table 1).

Structure activity relationship (SAR) study of the synthesized derivatives was performed by investigating the alteration in nature and position of involved groups or substituents (R) on the benzene rings. Compound **20** ($IC_{50}$ = 12 ± 0.9 μM) was found to be the supreme effective inhibitor of urease enzyme. The potency of compound **20** might be due to the attachment of the methoxy (–$OCH_3$) group at the *ortho* position of the benzene ring (Fig. 2).

Comparing compounds **16** ($IC_{50}$ = 13 ± 0.2 μM) and **32** ($IC_{50}$ = 15 ± 0.3 μM) with **8** ($IC_{50}$ = 41 ± 1.2 μM), the higher activity of **16** and **32** may perhaps be of nitro group at *para* and *ortho* positions attached to the ring of the benzene moiety. The compound **8** having less activity might be due to the nitro group attached to the *meta* position of the benzene ring (Fig. 3).

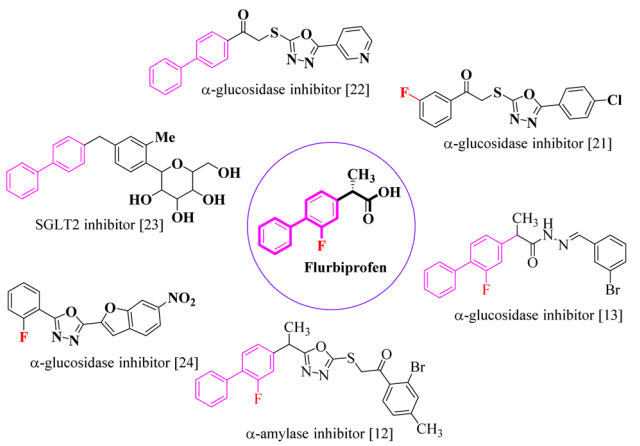


Fig. 1 Justification of the current study.

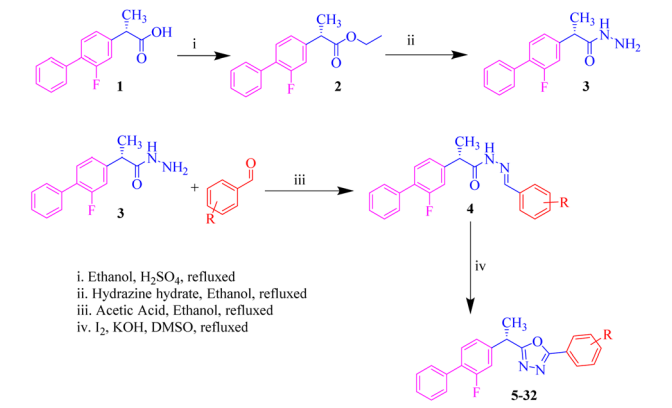


Scheme 1 Numerous replaced oxadiazole products based on flurbiprofen (**5–32**).

Table 1 Urease Inhibition Activity of Compounds (5–32)

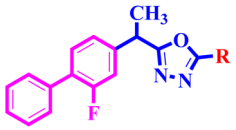


| Compd | R | $IC_{50} \pm SEM$ (μM) | Compd | R | $IC_{50} \pm SEM$ (μM) |
|---|---|---|---|---|---|
| **5** |  | 39 ± 1.2 | **19** | 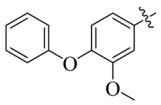 | 16 ± 0.3 |
| **6** | 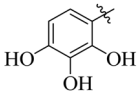 | 20 ± 0.5 | **20** | 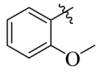 | 12 ± 0.9 |
| **7** | 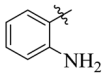 | 16 ± 0.1 | **21** | 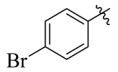 | 13 ± 0.2 |
| **8** | 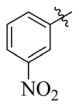 | 41 ± 1.2 | **22** | 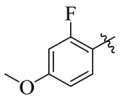 | 31 ± 1.4 |
| **9** | 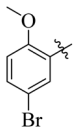 | 72 ± 1.2 | **23** | 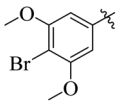 | 37 ± 1.4 |
| **10** | 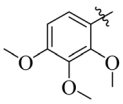 | 20 ± 0.5 | **24** | 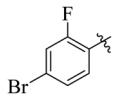 | 13 ± 0.1 |
| **11** | 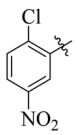 | 41 ± 1.2 | **25** | 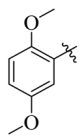 | 35 ± 1.5 |
| **12** | 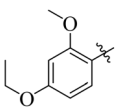 | 74 ± 1.3 | **26** | 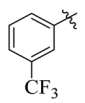 | 12 ± 0.1 |
| **13** | 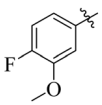 | 16 ± 0.9 | **27** | 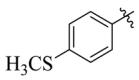 | 34 ± 2.4 |
| **14** | 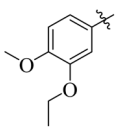 | 35 ± 1.2 | **28** | 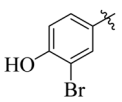 | 14 ± 0.3 |
| **15** | 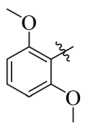 | 31 ± 1.2 | **29** | 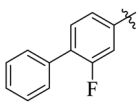 | 41 ± 1.4 |
| **16** | 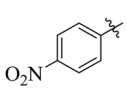 | 13 ± 0.2 | **30** | 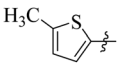 | 12 ± 0.1 |

Table 1 (*Contd.*)

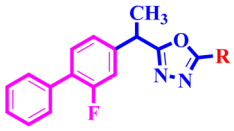

| Compd | R | $IC_{50}$ ± SEM (μM) | Compd | R | $IC_{50}$ ± SEM (μM) |
|---|---|---|---|---|---|
| **17** | 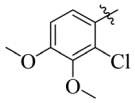 | 36 ± 1.2 | **31** | 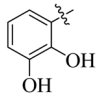 | 15 ± 0.3 |
| **18** | 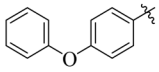 | 38 ± 1.4 | **32** | 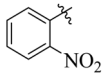 | 15 ± 0.3 |

**Thiourea** 22 ± 2.2 μM

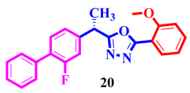


Fig. 2 Structure of the most potent urease inhibitor **20**.

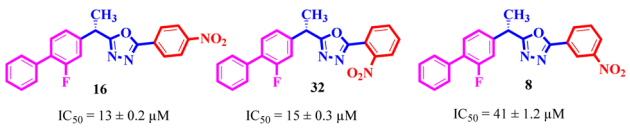


Fig. 3 Structure activity relationship comparison of compounds **16**, **32**, and **8**.

If we compare compounds **18** with **19** having $IC_{50}$ values of 38 ± 1.4 and 16 ± 0.3 μM, respectively, the higher activity of compound **16** could be due to the presence of the methoxy group at the *meta* position of the benzene ring. Addition of the electron donating methoxy group to compound **19** at the *meta* position significantly increases the activity of the compound (Fig. 4).

Similarly, by comparing compound **10** ($IC_{50}$ = 20 ± 0.5 μM) with **6** ($IC_{50}$ = 20 ± 0.5 μM), both derivatives showed excellent inhibitory potential better than the standard thiourea. The excellent activity of these compounds might be due to the presence of three electron donating groups attached at *ortho*, *meta*, and *para* positions of the benzene ring. A very slight decline occurs in the activity of compound **6** when the methoxy groups are replaced by hydroxyl groups at the same position (Fig. 5). It means that electron donating groups are responsible for enhancing the activity of the compounds against urease enzyme.

By comparing compound **14** with **12** with $IC_{50}$ values of 35 ± 1.2 and 74 ± 1.3 μM, respectively, the nature of attached substituents is the same but the positions are different. Amongst them, compound **14** showed excellent activity compared to **12**; the higher activity of this compound may be due to the presence of the ethoxy group at the *meta* position and the methoxy group at the *para* position of the benzene ring (Fig. 6). Transferring of the ethoxy group from *meta* to *para* and methoxy group from *para* to *ortho* group is responsible for the fall in activity of the compound.

### 2.3. Docking analysis

The docking results indicated that compounds **20**, **26**, **30**, **24**, **21**, **16**, **28**, **31**, **32**, **7**, **19**, **13**, **10**, and **6** had lower docking scores than the reference compound and revealed better interactions. The compounds were docked against the urease and a total of ten positions were nominated for every compound. The top-ranked posture for each compound was further designated for the interaction analysis. Among all the compounds of the series compound **20** was predicted as the most potent inhibitor of urease, followed by compound **26** based on the docking score. The docking score of compound **20** was predicted as −5.53 and formed a total of five interactions with the urease enzyme. Compound **20** formed a total of three H-donor interactions with

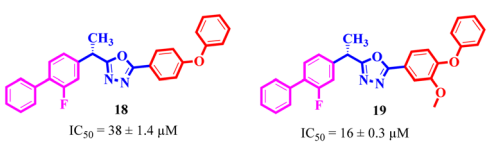


Fig. 4 Comparison of the structure activity relationship of compounds **18** and **19**.

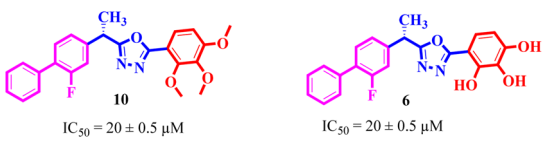


Fig. 5 Structure activity relationship study of compounds **10** and **6**.

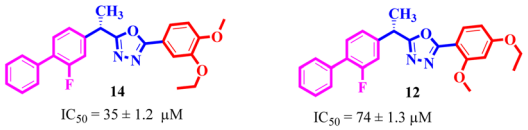


Fig. 6 Assessment of structure activity relationship study of compounds **14** and **12**.

Gly279 and Cys321 residues. Compound **20** also formed two pi-H interactions with Cys321. Most of the interactions were found within the active site residues of the urease. The docking score of compound **26** was predicted to be −5.18 and compound **26** formed a total of four interactions with the urease enzyme. Compound **26** formed two H-donor interactions with the Cys321 residue. The 6-ring of compound **26** established two pi-H interactions with the Gln364 and Ala365 residues of the receptor. Compounds **20**, **26**, **30**, **24**, **21**, **16**, **28**, **31**, **32**, **7**, **19**, **13**, **10**, and **6** were found most potent compared to the reference compound thiourea in terms of docking score and interactions. Table 2 describes the docking scores and interactions of the most potent compounds as well as the reference compound. Fig. 7 displays the three dimensional interactions of the most potent compounds such as compounds **20** and **26** along with the reference compounds within the active site of the urease enzyme.

### 2.4. Docking validation

To validate the docking protocol of MOE software the co-crystallized ligand (PDB ID; 6ZO1) was removed from the active site and re-docked into the binding site of the urease enzyme. The RMSD value between the top-ranked docked conformation and the co-crystallized ligand was predicted to be 1.3 Å (Fig. 8), revealing the validity of the MOE docking protocol.

## 3. Experimental

### 3.1. Materials and methods

Chemicals including reagents and solvents bought from BDH, Merck, and TCI were extra pure and utilized after receiving. Numerous substituted aldehydes (aromatic) and the starting material (*S*)-flurbiprofen having CAS No: 51543-39-6 and optical rotation were obtained from Sigma Aldrich. Dual wavelength ultra violet (UV) light of 254 and 365 nm was used for visualization of spots and aluminum cards (Merck, Kieselgel 60, GF254) were used for checking the direction of the desired reactions. Optical rotation was measured on an ATAGO, POLAX-2L polarimeter. Structure confirmation ($^1$H and $^{13}$C NMR) was carried out on an Avance-Bruker 400 MHz spectrophotometer, whereas molecular masses of the obtained products were established *via* High Resolution Electro Spray Ionization Mass Spectrometry (HR-ESI-MS). CHN analyses were carried out on a Carlo Erba Strumentazione-Mod-1106, Italy.

**3.1.1. Iodine mediated synthesis of oxadiazole derivatives (5–32) *via* cyclo addition reaction.** Flurbiprofen hydrazides (**3**) (2 mmol) and a number of substituted aromatic aldehydes (2 mmol) were mixed in 10 ml pure ethanol used as a solvent and catalyst acetic acid in little quantity. The reaction (mixture) was stirred through continuous heating for 4–5 hours. At the end of the chemical reaction, products obtained after filtration were washed with hot water and *n*-hexane to eradicate extra aldehydes and dried out in reduced pressure.[11] The obtained hydrazones of flurbiprofen were cyclized through iodine and potassium hydroxide in DMSO solvent. In a typical procedure, the obtained hydrazone Schiff base was dissolved in 15 ml DMSO and iodine (1.2 eq.) and KOH (3 eq.) were added to the reaction mixture. The reaction mixture was refluxed for 1–4 h with constant stirring. The improvement of reaction was tested with the help of thin layer chromatography (TLC) using a solvent system of *n*-hexane and ethyl acetate (7 : 3). After completion of the reaction, the mixture was poured into a beaker having icy distilled water. The mixture was treated with 5% $Na_2S_2O_3$ solution to remove the remaining iodine and extracted three times (3 × 30 ml) with an organic solvent through a separating funnel. The organic layer was dried under air, precipitates were formed, and the products were recrystallized with absolute ethanol to get pure oxadiazole derivatives of flurbiprofen. The synthesized analogues were confirmed with the help of HR-ESI-MS and $^1$H-NMR spectroscopy.

### 3.2. Urease inhibition assay (*in vitro*)

Urease inhibition potential of oxadiazole products was studied according to the described technique in the literature.[25–27] Concisely, 40 μL buffers, 10 μL of the blended products and 10 μL of enzyme (5 U ml$^{-1}$) were gestated for 10 minutes at 37 °C, in a 96 well plate. To each well, 40 μL of alkaline and phenolic reagents was added. Experiments were performed in triplicate. Absorbance was monitored at 625 *nm* with a microplate reader (Bio-TekELx 800, Instruments, Inc., USA). The standard inhibitor in this case was thiourea. The % inhibition was calculated by the use of the equation given below.

$$\% \text{ Inhibition} = (\text{absorbance control} - \text{absorbance sample})/\text{absorbance control} \times 100$$

The $IC_{50}$ values, and concentration needed for the inhibition of activity by 50% were determined using a non-linear regression graph, in which % inhibition of α-amylase (taken on the *x*-axis) was plotted against concentrations (taken on the *y*-axis). For this purpose GraphPad Prism Software (Version 7) was used.

### 3.3. Molecular docking

To carry out the molecular docking study low-resolution 3D structure of the urease enzyme [PDB code: 6ZO1] was retrieved from the PDB database.[28] The water was removed from the crystal structure and hydrogen was added to the structure. Based on the Amber99 force field charges were assigned to all atoms.[29] To draw the structures of compounds ChemDraw software was used and compounds were saved in the MDB database. The compounds were docked against the urease enzyme using the triangle matcher algorithm of the MOE software. For each compound, a total of ten poses were generated. The compounds were then ranked on the basis of the *S* score.

Table 2 Docking score and interactions of most potent compounds of the series

| C. no. | Ligand | Receptor | Interacting residues | Interaction type | Distance | Energy | *S* score |
|---|---|---|---|---|---|---|---|
| **20** | C 25 | O | GLY 279 | H-Donor | 3.59 | −1.1 | −5.53 |
| | O 32 | SG | CYS 321 | H-Donor | 3.91 | −0.1 | |
| | C 34 | SG | CYS 321 | H-Donor | 3.05 | −1.2 | |
| | 6-Ring | CB | CYS 321 | Pi-H | 4.64 | −0.1 | |
| | 6-Ring | CB | CYS 321 | Pi-H | 3.76 | −0.5 | |
| **26** | C 34 | SG | CYS 321 | H-Donor | 3.92 | −0.7 | −5.18 |
| | F 45 | SG | CYS 321 | H-Donor | 3.71 | −0.3 | |
| | 6-Ring | CB | GLN 364 | Pi-H | 4.52 | −0.5 | |
| | 6-Ring | CA | ALA 365 | Pi-H | 4.54 | −0.9 | |
| **30** | C 25 | O | GLY 279 | H-Donor | 3.72 | −0.1 | −4.36 |
| | N 29 | NI | NI 601 | H-Acceptor | 2.67 | −0.2 | |
| | N 30 | NI | NI 601 | Metal | 2.49 | −0.8 | |
| | C 14 | 5-Ring | HIS 322 | H-Pi | 4.49 | −0.1 | |
| | 6-Ring | CB | CYS 321 | Pi-H | 3.92 | −0.6 | |
| **24** | C 14 | OE1 | GLU 222 | H-Donor | 3.29 | −0.3 | −4.04 |
| | C 22 | OD1 | ASP 223 | H-Donor | 2.98 | −0.3 | |
| | BR 43 | O | HIS 314 | H-Donor | 3.59 | −0.7 | |
| | 5-Ring | CE1 | HIS 221 | Pi-H | 4.71 | −0.2 | |
| **21** | BR 43 | O | HIS 314 | H-Donor | 3.39 | −0.4 | −4.15 |
| | N 29 | CG2 | THR 251 | H-Acceptor | 4.16 | −0.1 | |
| | N 30 | CG2 | THR 251 | H-Acceptor | 4.26 | −0.1 | |
| | 6-Ring | CA | CYS 321 | Pi-H | 3.90 | −0.3 | |
| | 6-Ring | CB | CYS 321 | Pi-H | 3.80 | −0.4 | |
| | 5-Ring | CB | CYS 321 | Pi-H | 4.07 | −0.1 | |
| **16** | C 11 | SG | CYS 321 | H-Donor | 3.69 | −0.3 | −4.13 |
| | C 14 | SG | CYS 321 | H-Donor | 3.63 | −0.5 | |
| | O 20 | SG | CYS 321 | H-Donor | 3.53 | −0.2 | |
| | C 26 | SG | CYS 321 | H-Donor | 4.45 | −0.2 | |
| **28** | C 22 | OE1 | GLU 222 | H-Donor | 3.57 | −0.3 | −4.11 |
| | C 25 | OD2 | ASP 223 | H-Donor | 3.62 | −0.2 | |
| | O 42 | SD | MET 317 | H-Donor | 4.02 | −0.2 | |
| | N 30 | NH2 | ARG 338 | H-Acceptor | 3.06 | −0.3 | |
| | 6-Ring | CB | CYS 321 | Pi-H | 3.93 | −0.2 | |
| | 6-Ring | NE2 | HIS 323 | Pi-H | 3.74 | −0.2 | |
| **31** | C 17 | SG | CYS 321 | H-Donor | 3.59 | −0.3 | −3.97 |
| | C 25 | SG | CYS 321 | H-Donor | 3.95 | −0.2 | |
| | N 29 | NH2 | ARG 338 | H-Acceptor | 3.51 | −0.5 | |
| | 6-Ring | CB | MET 317 | Pi-H | 4.35 | −0.3 | |
| **32** | O 32 | SG | CYS 321 | H-Donor | 3.07 | −0.3 | −4.68 |
| | C 37 | O | HIS 314 | H-Donor | 3.42 | −0.3 | |
| | N 30 | NI | NI 601 | Metal | 2.61 | −2.0 | |
| | O 44 | NI | NI 601 | Metal | 2.57 | −1.2 | |
| | 6-Ring | CB | ASP 165 | Pi-H | 4.80 | −0.3 | |
| **7** | N 43 | SG | CYS 321 | H-Donor | 4.06 | −0.5 | −4.80 |
| | N 29 | NI | NI 601 | H-Acceptor | 2.70 | −0.2 | |
| | N 30 | NI | NI 601 | Metal | 2.51 | −1.4 | |
| | 6-Ring | CE1 | HIS 221 | Pi-H | 4.71 | −0.4 | |
| | 6-Ring | CB | CYS 321 | Pi-H | 4.07 | −0.2 | |
| **19** | C 14 | OE1 | GLU 222 | H-Donor | 3.46 | −0.2 | −4.25 |
| | C 22 | OE1 | GLU 222 | H-Donor | 3.63 | −0.2 | |
| | C 25 | OD1 | ASP 223 | H-Donor | 3.42 | −0.2 | |
| | 6-Ring | CB | CYS 321 | Pi-H | 4.28 | −0.2 | |
| | 6-Ring | NE2 | HIS 323 | Pi-H | 3.79 | −0.4 | |
| **13** | C 25 | SG | CYS 321 | H-Donor | 3.98 | −0.3 | −3.77 |
| | C 36 | OD2 | ASP 223 | H-Donor | 3.38 | −0.9 | |
| | C 40 | SG | CYS 321 | H-Donor | 3.65 | −0.5 | |
| | 6-Ring | CB | MET 317 | Pi-H | 4.66 | −0.5 | |
| **10** | C 19 | O | GLN 364 | H-Donor | 3.41 | −0.2 | −3.58 |
| | C 52 | O | ASN 168 | H-Donor | 3.43 | −0.2 | |
| | O 41 | NI | NI 601 | Metal | 2.51 | −0.2 | |
| | 6-Ring | CB | CYS 321 | Pi-H | 3.77 | −0.2 | |
| **6** | O 32 | SG | CYS 321 | H-Donor | 3.41 | −0.2 | −3.29 |

Table 2 (*Contd.*)

| C. no. | Ligand | Receptor | Interacting residues | Interaction type | Distance | Energy | *S* score |
|---|---|---|---|---|---|---|---|
| | N 29 | CB | ALA 169 | H-Acceptor | 3.37 | −0.2 | |
| | O 41 | NH2 | ARG 338 | H-Acceptor | 2.84 | −0.4 | |
| | 6-Ring | CB | CYS 321 | Pi-H | 4.41 | −0.1 | |
| | 6-Ring | NE2 | HIS 323 | Pi-H | 3.71 | −0.5 | |
| **Thiourea** | N 3 | O | ALA 278 | H-Donor | 3.08 | −1.6 | −3.19 |
| | S 1 | CA | GLY 279 | H-Acceptor | 3.67 | −1.0 | |
| | S 1 | NH2 | ARG 338 | H-Acceptor | 3.78 | −0.9 | |

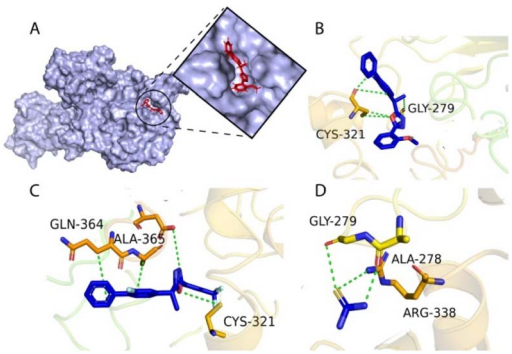


Fig. 7 (A) Active site of urease enzyme, and (B) 3D interaction of compound **20**, (C) compound **26**, and (D) reference compound with urease enzyme. Compounds are shown as blue sticks, while the green dotted lines represent bonds.

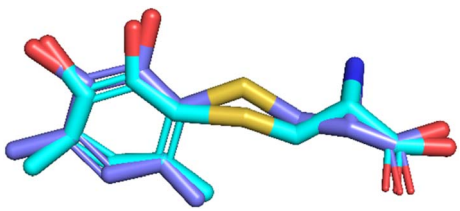

Fig. 8 Superposition of co-crystallized and docked conformations of the ligand. The purple colour represents the native co-crystallized ligand and the cyan colour is the docked ligand.

Thiourea was employed as the positive control. PyMol software was then used to generate the 3D interactions[30] of compounds in complex with urease.

### 3.4. Spectral data of the synthesized oxadiazole derivatives (5–32)

**3.4.1. 2-(1-(2-Fluoro-[1,1′-biphenyl]-4-yl)ethyl)-5-(naphthalen-1-yl)-1,3,4-oxadiazole (5).** Snowy amorphous solid; yield: 88%; $^1$H-NMR (400 MHz, $CDCl_3$; $\delta$, ppm): 1.31 (d, $J$ = 6.40 Hz, 3H), 3.83 (d, $J$ = 7.12 Hz, 1H), 7.47–7.60 (m, 5H), 7.62–7.72 (m, 5H), 7.74 (t, $J$ = 8.2 Hz, 1H), 8.10 (d, $J$ = 8.2 Hz, 1H), 8.26 (d, $J$ = 7.8 Hz, 1H), 8.63 (s, 1H), 9.29 (d, $J$ = 8.2 Hz, 1H); $^{13}$C-NMR (150 MHz, DMSO-$d_6$) $\delta$ 21.4 (1C), 42.7 (1C), 114.4 (1C), 121.3 (1C), 123.7 (1C), 125.9 (1C), 126.7 (2C), 127.1 (1C), 127.8 (5C), 128.2 (1C), 128.5 (3C), 130.0 (1C), 131.9 (1C), 133.8 (1C), 136.5 (1C), 141.2 (1C), 157.7 (1C), 166.8 (1C), 173.3 (1C); HR-ESI-MS [M + H]$^+$ calculated for $C_{26}H_{19}FN_2O$, 394.1481, found 394.4403; anal. calcd for $C_{26}H_{19}FN_2O$ (394.15): C, 79.17; H, 4.86; F, 4.82; N, 7.10; O, 4.06; found: C, 79.18; H, 4.84; N, 7.11.

**3.4.2. 4-(5-(1-(2-Fluoro-[1,1′-biphenyl]-4-yl)ethyl)-1,3,4-oxadiazol-2-yl) benzene-1,2,3-triol (6).** White amorphous solid; yield: 85%; $^1$H-NMR (400 MHz, $CDCl_3$; $\delta$, ppm): 1.63 (d, $J$ = 7.1 Hz, 3H), 3.86 (d, $J$ = 7.1 Hz, 1H), 7.22 (t, $J$ = 7.9 Hz, 2H), 7.51–7.40 (m, 6H), 7.59 (d, $J$ = 8.0 Hz, 1H); $^{13}$C-NMR (150 MHz, DMSO-$d_6$) $\delta$ 20.2 (1C), 40.7 (1C), 108.5 (1C), 114.4 (1C), 115.8 (1C), 126.2 (1C), 127.7 (4C), 128.2 (1C), 128.8 (2C), 130.9 (1C), 132.7 (1C), 136.5 (1C), 141.2 (1C), 146.8 (1C), 150.0 (1C), 160.1 (1C), 165.2 (1C), 173.3 (1C); HR-ESI-MS [M + H]$^+$ calculated for $C_{22}H_{17}FN_2O_4$, 392.1172, found 392.1172; anal. calcd for $C_{22}H_{17}FN_2O_4$ (392.12) C, 67.34; H, 4.37; F, 4.84; N, 7.14; O, 16.31; found: C, 67.35; H, 4.39; N, 7.12.

**3.4.3. 2-(5-(1-(2-Fluoro-[1,1′-biphenyl]-4-yl)ethyl)-1,3,4-oxadiazol-2-yl) aniline (7).** Silvery amorphous solid; yield: 82%; $^1$H-NMR (400 MHz, $CDCl_3$; $\delta$, ppm): 1.31 (d, $J$ = 7.1 Hz, 3H), 2.69 (q, $J$ = 7.0 Hz, 1H), 7.41–7.45 (m, 3H), 7.51–7.58 (m, 4H), 7.80–7.87 (m, 3H), 8.05–8.10 (m, 2H); $^{13}$C-NMR (150 MHz, DMSO-$d_6$) $\delta$ 19.1 (1C), 42.3 (1C), 108.4 (1C), 113.4 (1C), 115.2 (1C), 126.2 (1C), 127.7 (3C), 128.1 (2C), 128.7 (3C), 129.3 (1C), 131.9 (1C), 136.5 (1C), 141.2 (1C), 150.1 (1C), 159.9 (1C), 165.2 (1C), 172.1 (1C); HR-ESI-MS [M + H]$^+$ calculated for $C_{22}H_{18}FN_3O$, 359.1434, found 359.3962; anal. calcd for $C_{22}H_{18}FN_3O$ (359.14) C, 73.52; H, 5.05; F, 5.29; N, 11.69; O, 4.45; found: C, 73.50; H, 5.03; N, 11.71.

**3.4.4. 2-(1-(2-Fluoro-[1,1′-biphenyl]-4-yl)ethyl)-5-(3-nitrophenyl)-1,3,4-oxadiazole (8).** Off-white amorphous solid; yield: 80%; $^1$H-NMR (400 MHz, $CDCl_3$; $\delta$, ppm): 1.45 (d, $J$ = 7.1 Hz, 3H), 3.61 (q, $J$ = 7.1 Hz, 1H), 7.30–7.32 (m, 5H), 7.58 (d, $J$ = 7.9 Hz, 1H), 7.80 (d, $J$ = 7.1 Hz, 1H), 7.85–7.83 (m, 2H), 8.14 (d, $J$ = 8.3 Hz, 1H), 8.35 (t, $J$ = 8.4 Hz, 1H), 8.61 (d, $J$ = 8.3 Hz, 1H); $^{13}$C-NMR (150 MHz, DMSO-$d_6$) $\delta$ 21.9 (1C), 42.5 (1C), 113.4 (1C), 116.7 (1C), 118.3 (1C), 125.0 (1C), 126.1 (1C), 127.0 (1C), 127.8 (3C), 128.2 (1C), 128.8 (2C), 129.2 (1C), 130.9 (1C), 136.5 (1C), 140.2 (1C), 140.5 (1C), 161.7 (1C), 164.2 (1C), 173.3 (1C); HR-ESI-MS [M + H]$^+$ calculated for $C_{22}H_{16}FN_3O_3$, 389.1176, found 389.3791; anal. calcd for $C_{22}H_{16}FN_3O_3$ (389.12) C, 67.86; H, 4.14; F, 4.88; N, 10.79; O, 12.33; found: C, 67.87; H, 4.17; N, 10.80.

**3.4.5. 2-(5-Bromo-2-methoxyphenyl)-5-(1-(2-fluoro-[1,1′-biphenyl]-4-yl) ethyl)-1,3,4-oxadiazole (9).** Ash-white amorphous

solid; yield: 84%; $^1$H-NMR (400 MHz, $CDCl_3$; $\delta$, ppm): 1.48 (d, $J$ = 7.2 Hz, 3H), 3.51 (q, $J$ = 7.2 Hz, 1H), 3.62 (s, 3H), 6.93–9.99 (m, 3H), 7.37–7.43 (m, 2H), 7.44–7.49 (m, 5H), 7.58–7.64 (m, 2H); $^{13}$C-NMR (150 MHz, DMSO-$d_6$) $\delta$ 18.9 (1C), 42.1 (1C), 58.0 (1C), 108.5 (1C), 112.1 (1C), 116.4 (1C), 119.4 (1C), 126.2 (1C), 127.8 (3C), 128.0 (1C), 128.4 (2C), 129.9 (1C), 131.0 (1C), 132.7 (1C), 136.5 (1C), 141.2 (1C), 158.7 (1C), 161.3 (1C), 162.2 (1C), 171.1 (1C); HR-ESI-MS [M + H]$^+$ calculated for $C_{23}H_{18}BrFN_2O_2$, 452.0536, found 453.3036; anal. calcd for $C_{23}H_{18}BrFN_2O_2$ (552.05) C, 60.94; H, 4.00; Br, 17.63; F, 4.19; N, 6.18; O, 7.06; found: C, 60.97; H, 4.02; N, 6.19.

**3.4.6. 2-(2,3,4-Trimethoxyphenyl)-5-(1-(2-fluoro-[1,1′-biphenyl]-4-yl) ethyl)-1,3,4-oxadiazole (10).** Off-white amorphous solid; yield: 80%; $^1$H-NMR (400 MHz, $CDCl_3$; $\delta$, ppm): 3.98 (q, $J$ = 7.1 Hz, 1H), 3.93 (s, 3H), 3.96 (s, 3H), 3.97 (s, 3H), 4.12 (d, $J$ = 7.1 Hz, 3H), 6.83 (d, $J$ = 7.2 Hz, 1H), 7.40–7.44 (m, 2H), 7.45–7.52 (m, 4H), 7.57–7.59 (m, H), 7.69 (d, $J$ = 7.2 Hz, 1H); $^{13}$C-NMR (150 MHz, DMSO-$d_6$) $\delta$ 21.3 (1C), 40.7 (1C), 57.0 (3C), 111.5 (1C), 111.8 (1C), 116.4 (1C), 126.2 (1C), 127.8 (4C), 128.0 (1C), 128.4 (2C), 131.9 (1C), 136.7 (1C), 138.2 (1C), 141.4 (1C), 144.4 (1C), 156.5 (1C), 160.7 (1C), 165.2 (1C), 172.3 (1C); HR-ESI-MS [M + H]$^+$ calculated for $C_{25}H_{23}FN_2O_4$, 434.1642, found 434.4702; anal. calcd for $C_{25}H_{23}FN_2O_4$ (434.16) C, 69.11; H, 5.34; F, 4.37; N, 6.45; O, 14.73; found: C, 69.13; H, 4.37; N, 6.44.

**3.4.7. 2-(2-Chloro-5-nitrophenyl)-5-(1-(2-fluoro-[1,1′-biphenyl]-4-yl) ethyl)-1,3,4-oxadiazole (11).** Snowy white amorphous solid; yield: 85%; $^1$H-NMR (400 MHz, $CDCl_3$; $\delta$, ppm): 1.34 (d, $J$ = 7.2 Hz, 3H), 3.47 (q, $J$ = 7.4 Hz, 1H), 7.47–7.60 (m, 9H), 7.63–7.78 (m, 1H), 7,87 (d, $J$ = 8.5 Hz, 1H); $^{13}$C-NMR (150 MHz, DMSO-$d_6$) $\delta$ 19.5 (1C), 40.7 (1C), 115.2 (1C), 117.1 (1C), 119.5 (1C), 127.6 (1C), 127.7 (3C), 128.0 (1C), 128.2 (1C), 128.4 (2C), 130.9 (1C), 131.3 (1C), 133.2 (1C), 135.5 (1C), 139.2 (1C), 139.9 (1C), 159.3 (1C), 163.6 (1C), 171.1 (1C); HR-ESI-MS [M + H]$^+$ calculated for $C_{22}H_{15}ClFN_3O_3$, 423.0786, found 423.8242; anal. calcd for $C_{22}H_{15}ClFN_3O_3$ (423.08) C, 62.35; H, 3.57; Cl, 8.37; F, 4.48; N, 9.91; O, 11.33; found: C, 62.33; H, 3.59; N, 9.90.

**3.4.8. 2-(4-Ethoxy-2-methoxyphenyl)-5-(1-(2-fluoro-[1,1′-biphenyl]-4-yl) ethyl)-1,3,4-oxadiazole (12).** White amorphous solid; yield: 78%; $^1$H-NMR (400 MHz, $CDCl_3$; $\delta$, ppm): 1.49 (d, $J$ = 6.8 Hz, 3H), 1.58 (t, $J$ = 6.8 Hz, 3H), 4.01 (s, 3H), 4.24 (q, $J$ = 6.8 Hz, 1H), 4.23 (q, $J$ = 6.6 Hz, 2H), 7.02 (d, $J$ = 7.2 Hz, 1H), 7.31 (s, 1H), 7.46–7.68 (m, 8H), 8.47 (m, 1H); $^{13}$C-NMR (150 MHz, DMSO-$d_6$) $\delta$ 14.2 (1C), 18.1 (1C), 42.7 (1C), 56.0 (1C), 64.3 (1C), 98.7 (1C), 110.5 (1C), 112.3 (1C), 114.4 (1C), 127.2 (1C), 127.6 (4C), 128.1 (1C), 128.4 (2C), 131.9 (1C), 134.5 (1C), 138.2 (1C), 155.3 (1C), 158.7 (1C), 160.9 (1C), 165.2 (1C), 173.3 (1C); HR-ESI-MS [M + H]$^+$ calculated for $C_{25}H_{23}FN_2O_3$, 418.1693, found 418.4601; anal. calcd for $C_{25}H_{23}FN_2O_3$ (418.17) C, 71.76; H, 5.54; F, 4.54; N, 6.69; O, 11.47; found: C, 71.8; H, 5.55; N, 6.67.

**3.4.9. 2-(4-Fluoro-3-methoxyphenyl)-5-(1-(2-fluoro-[1,1′-biphenyl]-4-yl) ethyl)-1,3,4-oxadiazole (13).** Off white amorphous solid; yield: 88%; $^1$H-NMR (400 MHz, $CDCl_3$; $\delta$, ppm): 1.35 (d, $J$ = 7.0 Hz, 3H), 3.97 (q, $J$ = 7.1 Hz, 1H), 4.01 (s, 3H), 7.26 (t, $J$ = 7.4 Hz, 1H), 7.31 (s, 1H), 7.43–7.51 (m, 4H), 7.57 (d, $J$ = 7.4 Hz, 1H), 7.67–7.71 (m, 1H), 7.70 (d, $J$ = 8.0 Hz, 1H); $^{13}$C-NMR (150 MHz, DMSO-$d_6$) $\delta$ 20.3 (1C), 40.7 (1C), 56.0 (1C), 110.6 (1C), 115.4 (1C), 117.7 (1C), 126.0 (1C), 127.2 (1C), 127.5 (3C), 128.6 (1C), 128.8 (2C), 131.9 (1C), 133.4 (1C), 136.5 (1C), 140.2 (1C), 147.7 (1C), 153.9 (1C), 158.7 (1C), 164.2 (1C), 172.3 (1C); HR-ESI-MS [M + H]$^+$ calculated for $C_{23}H_{18}F_2N_2O_2$, 392.1386, found 392.1342; anal. calcd for $C_{23}H_{18}F_2N_2O_2$ (392.14) C, 70.40; H, 4.62; F, 9.68; N, 7.14; O, 8.15; found: C, 70.42; H, 4.63; N, 7.12.

**3.4.10. 2-(3-Ethoxy-4-methoxyphenyl)-5-(1-(2-fluoro-[1,1′-biphenyl]-4-yl)ethyl)-1,3,4-oxadiazole (14).** Off white amorphous solid; yield: 85%; $^1$H-NMR (400 MHz, $CDCl_3$; $\delta$, ppm): 1.43 (d, $J$ = 7.1 Hz, 3H), 1.81 (t, $J$ = 6.9 Hz, 3H), 3.45 (q, $J$ = 6.9 Hz, 1H), 3.61 (q, $J$ = 7.1 Hz, 2H), 3.66 (s, 3H), 7.14–7.17 (m, 5H), 7.25 (d, $J$ = 7.3 Hz, 1H), 7.32 (d, $J$ = 7.3 Hz, 2H), 7.51–7.53 (m, 3H); $^{13}$C-NMR (150 MHz, DMSO-$d_6$) $\delta$ 16.2 (1C), 19.7 (1C), 41.7 (1C), 56.4 (1C), 64.5 (1C), 111.6 (1C), 112.2 (1C), 115.4 (1C), 125.0 (1C), 127.2 (1C), 127.8 (3C), 128.4 (2C), 129.2 (1C), 131.9 (1C), 136.5 (1C), 140.2 (1C), 148.4 (1C), 148.9 (1C), 160.7 (1C), 164.2 (1C), 172.3 (1C); HR-ESI-MS [M + H]$^+$ calculated for $C_{25}H_{23}FN_2O_3$, 418.1693, found 418.4601; anal. calcd for $C_{25}H_{23}FN_2O_3$ (418.17) C, 71.76; H, 5.54; F, 4.54; N, 6.69; O, 11.47; found: C, 71.77; H, 5.52; N, 6.71.

**3.4.11. 2-(2,6-Dimethoxyphenyl)-5-(1-(2-fluoro-[1,1′-biphenyl]-4-yl)ethyl)-1,3,4-oxadiazole (15).** White amorphous solid; yield: 88%; $^1$H-NMR (400 MHz, $CDCl_3$; $\delta$, ppm): 1.42 (d, $J$ = 7.0 Hz, 3H), 3.40 (q, $J$ = 7.0 Hz, 1H), 3.69 (s, 6H), 7.10–7.12 (m, 5H), 7.27 (t, $J$ = 7.0 Hz, 1H), 7.30 (d, $J$ = 7.0 Hz, 2H), 7.52–7.55 (m, 3H); $^{13}$C-NMR (150 MHz, DMSO-$d_6$) $\delta$ 21.3 (1C), 40.7 (1C), 56.8 (2C), 114.4 (1C), 115.8 (2C), 120.9 (1C), 126.2 (1C), 127.8 (3C), 128.6 (1C), 128.4 (2C), 130.9 (1C), 131.2 (1C), 134.5 (1C), 138.2 (1C), 156.8 (2C), 159.7 (1C), 165.2 (1C), 173.3 (1C); HR-ESI-MS [M + H]$^+$ calculated for $C_{24}H_{21}FN_2O_3$, 404.1536, found 404.4335; anal. calcd for $C_{24}H_{21}FN_2O_3$ (404.15) C, 71.27; H, 5.23; F, 4.70; N, 6.93; O, 11.87; found: C, 71.28; H, 5.25; N, 6.91.

**3.4.12. 2-(1-(2-Fluoro-[1,1′-biphenyl]-4-yl)ethyl)-5-(4-nitrophenyl)-1,3,4-oxadiazole (16).** White amorphous solid; yield: 80%; $^1$H-NMR (400 MHz, $CDCl_3$; $\delta$, ppm): 1.44 (d, $J$ = 6.7 Hz, 3H), 3.41 (q, $J$ = 6.7 Hz, 1H), 7.11–7.13 (m, 5H), 7.52–7.55 (m, 3H), 7.73 (d, $J$ = 8.5 Hz, 2H), 8.67 (d, $J$ = 8.5 Hz, 2H); $^{13}$C-NMR (150 MHz, DMSO-$d_6$) $\delta$ 19.5 (1C), 40.9 (1C), 115.4 (1C), 116.6 (2C), 120.8 (1C), 127.0 (1C), 127.8 (3C), 128.2 (1C), 128.6 (2C), 129.4 (2C), 131.1 (1C), 136.3 (1C), 140.4 (1C), 139.3 (1C), 159.5 (1C), 163.8 (1C), 171.1 (1C); HR-ESI-MS [M + H]$^+$ calculated for $C_{22}H_{16}FN_3O_3$, 389.1176, found 389.1176; anal. calcd for $C_{22}H_{16}FN_3O_3$ (389.12) C, 67.86; H, 4.14; F, 4.88; N, 10.79; O, 12.33; found: C, 67.88; H, 4.11; N, 10.80.

**3.4.13. 2-(2-Chloro-3,4-dimethoxyphenyl)-5-(1-(2-fluoro-[1,1′-biphenyl]-4-yl)ethyl)-1,3,4-oxadiazole (17).** Off white amorphous solid; yield: 90%; $^1$H-NMR (400 MHz, $CDCl_3$; $\delta$, ppm): 1.65 (d, $J$ = 6.9 Hz, 3H), 3.89 (q, $J$ = 6.9 Hz, 1H), 3.94 (s, 3H), 3.98 (s, 3H), 6.96 (d, $J$ = 7.5 Hz, 1H), 7.30–7.47 (m, 5H), 7.58 (d, $J$ = 7.5 Hz, 1H), 7.77 (d, $J$ = 7.2 Hz, 1H), 8.12 (s, 1H), 9.04 (s, 1H); $^{13}$C-NMR (150 MHz, DMSO-$d_6$) $\delta$ 20.3 (1C), 41.1 (1C), 56.0 (2C), 110.2 (1C), 115.4 (1C), 120.0 (1C), 126.9 (1C), 127.9 (4C), 128.0 (1C), 128.2 (1C), 128.4 (2C), 130.9 (1C), 135.9 (1C), 137.2 (1C), 146.8 (1C), 155.1 (1C), 159.7 (1C), 165.2 (1C, s), 171.5 (1C); HR-ESI-MS [M + H]$^+$ calculated for $C_{24}H_{20}ClFN_2O_3$, 438.1142, found 438.1140; anal. calcd for $C_{24}H_{20}ClFN_2O_3$ (438.11) C, 65.68; H, 4.59; Cl, 8.08; F, 4.33; N, 6.38; O, 10.94; found: C, 65.66; H, 4.58; N, 6.40.

**3.4.14. 2-([1,1′-Biphenyl]-4-yl)-5-(1-(2-fluoro-[1,1′-biphenyl]-4-yl)ethyl)-1,3,4-oxadiazole (18).** Off white amorphous solid; yield: 88%; $^1$H-NMR (400 MHz, $CDCl_3$; $\delta$, ppm): 1.43 (d, $J$ = 7.1 Hz, 3H), 3.44 (q, $J$ = 7.1 Hz, 1H), 7.07–7.16 (m, 3H), 7.31 (d, $J$ = 7.0 Hz, 2H), 7.40–7.63 (m, 5H), 7.91 (d, $J$ = 8.0 Hz, 2H), 8.00–8.11 (m, 4H), 8.49 (d, $J$ = 8.0 Hz, 1H); $^{13}$C-NMR (150 MHz, DMSO-$d_6$) $\delta$ 19.9 (1C), 40.1 (1C), 112.3 (2C), 115.2 (1C), 116.3 (2C), 122.8 (1C), 127.0 (1C), 127.5 (4C), 128.0 (1C), 128.4 (2C), 129.0 (2C), 129.6 (2C), 131.9 (1C), 136.5 (1C), 140.2 (1C), 156.1 (2C), 160.3 (1C), 164.2 (1C), 172.3 (1C); HR-ESI-MS [M + H]$^+$ calculated for $C_{28}H_{21}FN_2O_2$, 436.1638, found 436.4775; anal. calcd for $C_{28}H_{21}FN_2O_2$ (436.16) C, 77.05; H, 4.85; F, 4.35; N, 6.42; O, 7.33; found: C, 77.07; H, 4.82; N, 6.40.

**3.4.15. 2-(1-(2-Fluoro-[1,1′-biphenyl]-4-yl)ethyl)-5-(3-methoxy-4-phenoxyphenyl)-1,3,4-oxadiazole (19).** White amorphous solid; yield: 90%; $^1$H-NMR (400 MHz, $CDCl_3$; $\delta$, ppm): 1.64 (d, $J$ = 7.0 Hz, 3H), 3.98 (s, 3H), 5.29 (q, $J$ = 7.0 Hz, 1H), 6.95 (d, $J$ = 7.6 Hz, 1H), 7.14 (d, $J$ = 8.0 Hz, 1H), 7.24–7.27 (m, 2H), 7.34–7.7.59 (m, 10H), 7.66 (s, 1H), 7.57–7.59 (m, 6H), 7.87 (t, $J$ = 7.0 Hz, 2H); $^{13}$C-NMR (150 MHz, DMSO-$d_6$) $\delta$ 19.9 (1C, s), 39.9 (1C), 56.6 (1C), 109.6 (1C), 111.4 (1C), 115.0 (1C), 116.3 (2C), 126.0 (1C), 127.3 (1C), 127.4 (4C), 128.0 (1C), 128.4 (2C), 129.0 (1C), 129.6 (2C), 131.9 (1C), 134.5 (1C), 140.2 (1C), 147.0 (1C), 148.2 (1C), 156.5 (1C), 159.9 (1C), 164.2 (1C), 173.3 (1C); HR-ESI-MS [M + H]$^+$ calculated for $C_{29}H_{23}FN_2O_2$, 466.1693, found 466.5035; anal. calcd for $C_{29}H_{23}FN_2O_2$ (466.17) C, 74.66; H, 4.97; F, 4.07; N, 6.00; O, 10.29; found: C, 74.69; H, 4.99; N, 6.02.

**3.4.16. 2-(1-(2-Fluoro-[1,1′-biphenyl]-4-yl)ethyl)-5-(2-methoxyphenyl)-1,3,4-oxadiazole (20).** White amorphous solid; yield: 92%; $^1$H-NMR (400 MHz, $CDCl_3$; $\delta$, ppm): 1.34 (d, $J$ = 7.0 Hz, 3H), 3.46 (q, $J$ = 7.0 Hz, 1H), 3.94 (s, 3H), 7.17–7.19 (m, 4H), 7.27 (d, $J$ = 7.6 Hz, 1H), 7.34 (t, $J$ = 7.6 Hz, 2H), 7.45 (d, $J$ = 7.6 Hz, 1H), 7.58–7.60 (m, 4H); $^{13}$C-NMR (150 MHz, DMSO-$d_6$) $\delta$ 19.1 (1C), 41.9 (1C), 56.4 (1C), 110.9 (1C), 115.8 (1C), 117.8 (1C), 125.9 (1C), 127.0 (1C), 127.6 (3C), 128.2 (1C), 128.5 (3C), 129.6 (1C), 131.9 (1C), 136.5 (1C), 139.6 (1C), 160.7 (1C), 162.1 (1C), 165.2 (1C), 171.9 (1C); HR-ESI-MS [M + H]$^+$ calculated for $C_{23}H_{19}FN_2O_2$, 374.1431, found 374.4076; anal. calcd for $C_{23}H_{19}FN_2O_2$ (374.14) C, 73.78; H, 5.11; F, 5.07; N, 7.48; O, 8.55; found: C, 73.80; H, 5.10; N, 7.51.

**3.4.17. 2-(4-Bromophenyl)-5-(1-(2-fluoro-[1,1′-biphenyl]-4-yl)ethyl)-1,3,4-oxadiazole (21).** White amorphous solid; yield: 85%; $^1$H-NMR (400 MHz, $CDCl_3$; $\delta$, ppm): 1.44 (d, $J$ = 6.8 Hz, 3H), 3.40 (q, $J$ = 6.8 Hz, 1H), 7.42–7.70 (m, 11H), 7.94 (d, $J$ = 8.0 Hz, 1H); $^{13}$C-NMR (150 MHz, DMSO-$d_6$) $\delta$ 19.9 (1C), 41.9 (1C), 114.4 (1C), 121.3 (1C), 122.8 (1C), 127.4 (1C), 127.9 (3C), 128.3 (1C), 128.7 (2C), 129.3 (2C), 130.7 (1C), 132.3 (2C), 135.5 (1C), 138.2 (1C), 160.5 (1C), 164.2 (1C), 172.1 (1C); HR-ESI-MS [M + H]$^+$ calculated for $C_{22}H_{16}BrFN_2O$, 422.0430, found 423.2776; anal. calcd for $C_{22}H_{16}BrFN_2O$ (422.04) C, 62.43; H, 3.81; Br, 18.88; F, 4.49; N, 6.62; O, 3.78; found: C, 62.44; H, 3.83; N, 6.64.

**3.4.18. 2-(2-Fluoro-4-methoxyphenyl)-5-(1-(2-fluoro-[1,1′-biphenyl]-4-yl)ethyl)-1,3,4-oxadiazole (22).** Yellowish amorphous solid; yield: 90%; $^1$H-NMR (400 MHz, $CDCl_3$; $\delta$, ppm): 1.38 (d, $J$ = 7.3 Hz, 3H), 3.46 (q, $J$ = 7.3 Hz, 1H), 3.91 (s, 3H), 7.25–7.27 (m, 5H), 7.45 (d, $J$ = 7.4 Hz, 1H), 7.49 (d, $J$ = 7.4 Hz, 2H), 7.51 (s, 1H), 7.59–7.61 (m, 2H); $^{13}$C-NMR (150 MHz, DMSO-$d_6$) $\delta$ 20.1 (1C), 41.7 (1C), 56.6 (1C), 102.5 (1C), 114.3 (1C), 115.4 (1C), 127.0 (1C), 127.5 (4C), 128.0 (1C), 128.2 (1C), 128.4 (2C), 131.3 (1C), 136.1 (1C), 139.4 (1C), 160.3 (1C), 160.6 (2C), 164.4 (1C), 171.5 (1C, s); HR-ESI-MS [M + H]$^+$ calculated for $C_{23}H_{18}F_2N_2O_2$, 392.1336, found 392.3980; anal. calcd for $C_{23}H_{18}F_2N_2O_2$ (392.13) C, 70.40; H, 4.62; F, 9.68; N, 7.14; O, 8.15; found: C, 70.43; H, 4.61; N, 7.12.

**3.4.19. 2-(4-Bromo-3,5-dimethoxyphenyl)-5-(1-(2-fluoro-[1,1′-biphenyl]-4-yl)ethyl)-1,3,4-oxadiazole (23).** Pale yellow amorphous solid; yield: 92%; $^1$H-NMR (400 MHz, $CDCl_3$; $\delta$, ppm): 1.43 (d, $J$ = 7.0 Hz, 3H), 3.44 (q, $J$ = 7.0 Hz, 1H), 3.91 (s, 3H), 3.92 (s, 3H), 7.29–7.32 (m, 5H), 7.38 (s, 2H), 7.60–7.62 (m, 3H); $^{13}$C-NMR (150 MHz, DMSO-$d_6$) $\delta$ 20.5 (1C), 39.7 (1C), 55.8 (2C), 106.0 (1C), 110.6 (2C), 114.4 (1C), 125.6 (1C), 127.0 (1C), 127.5 (3C), 128.0 (1C), 128.4 (2C), 131.1 (1C), 136.7 (1C), 138.9 (1C), 156.4 (2C), 159.5 (1C), 164.2 (1C), 172.3 (1C); HR-ESI-MS [M + H]$^+$ calculated for $C_{24}H_{19}BrF_2N_2O_3$, 482.0641, found 482.3296; anal. calcd for $C_{24}H_{19}BrF_2N_2O_3$ (482.06) C, 59.64; H, 4.17; Br, 16.53; F, 3.93; N, 5.80; O, 9.93; found: C, 59.66; H, 4.19; N, 5.77.

**3.4.20. 2-(4-Bromo-2-fluorophenyl)-5-(1-(2-fluoro-[1,1′-biphenyl]-4-yl)ethyl)-1,3,4-oxadiazole (24).** White amorphous solid; yield: 75%; $^1$H-NMR (400 MHz, $CDCl_3$; $\delta$, ppm): 1.31 (d, $J$ = 6.6 Hz, 3H), 3.49 (q, $J$ = 6.6 Hz, 1H), 7.45–7.53 (m, 7H), 7.61–7.63 (m, 2H), 8.03 (t, $J$ = 7.5 Hz, 1H), 8.59 (s, 1H); $^{13}$C-NMR (150 MHz, DMSO-$d_6$) $\delta$ 19.3 (1C), 40.3 (1C), 114.4 (1C), 119.5 (1C), 121.5 (1C), 127.0 (1C), 127.8 (4C), 128.0 (1C), 128.2 (1C), 128.4 (2C), 130.9 (1C), 131.5 (1C), 135.7 (1C), 140.4 (1C), 160.5 (1C), 161.9 (1C), 164.2 (1C), 172.5 (1C); HR-ESI-MS [M + H]$^+$ calculated for $C_{22}H_{15}BrF_2N_2O$, 440.0336, found 441.2681; anal. calcd for $C_{22}H_{15}BrF_2N_2O$ (440.03) C, 59.88; H, 3.43; Br, 18.11; F, 8.61; N, 6.35; O, 3.63; found: C, 59.89; H, 3.45; N, 6.35.

**3.4.21. 2-(2,5-Dimethoxyphenyl)-5-(1-(2-fluoro-[1,1′-biphenyl]-4-yl) ethyl)-1,3,4-oxadiazole (25).** White amorphous solid; yield: 78%; $^1$H-NMR (400 MHz, $CDCl_3$; $\delta$, ppm): 1.23 (d, $J$ = 6.7 Hz, 3H), 3.54 (q, $J$ = 6.7 Hz, 1H), 3.74 (s, 3H), 3.90 (s, 3H), 6.90 (d, $J$ = 7.0 Hz, 1H), 7.01–7.03 (m, 5H), 7.17 (s, 1H), 7.26 (d, $J$ = 7.0 Hz, 1H), 7.46–7.49 (m, 3H); $^{13}$C-NMR (150 MHz, DMSO-$d_6$) $\delta$ 19.7 (1C), 40.7 (1C), 56.0 (2C), 110.5 (2C), 112.5 (1C), 115.4 (2C), 127.2 (1C), 127.7 (3C), 128.4 (1C), 128.6 (2C), 131.7 (1C), 137.5 (1C), 141.4 (1C), 157.8 (1C), 160.65 (1C), 160.1 (1C), 164.2 (1C), 172.5 (1C); HR-ESI-MS [M + H]$^+$ calculated for $C_{24}H_{21}FN_2O_3$, 404.1536, found 404.1536; anal. calcd for $C_{24}H_{21}FN_2O_3$ (404.15) C, 71.27; H, 5.23; F, 4.70; N, 6.93; O, 11.87; found: C, 71.29; H, 5.24; N, 4.67.

**3.4.22. 2-(1-(2-Fluoro-[1,1′-biphenyl]-4-yl)ethyl)-5-(3-(trifluoromethyl) phenyl)-1,3,4-oxadiazole (26).** White amorphous solid; yield: 92%; $^1$H-NMR (400 MHz, $CDCl_3$; $\delta$, ppm): 1.58 (d, $J$ = 6.9 Hz, 3H), 2.69 (q, $J$ = 6.9 Hz, 1H), 7.31–7.62 (m, 5H), 7.68–7.80 (m, 3H), 7.78 (d, $J$ = 7.5 Hz, 1H), 7.87 (d, $J$ = 8.5 Hz, 1H), 8.19 (t, $J$ = 8.5 Hz, 1H), 8.29 (d, $J$ = 8.5 Hz, 1H); $^{13}$C-NMR (150 MHz, DMSO-$d_6$) $\delta$ 19.3 (1C), 40.7 (1C), 115.4 (1C), 123.7 (2C), 126.2 (1C), 126.5 (1C), 127.2 (1C), 127.4 (1C), 127.8 (3C), 128.0 (1C), 128.2 (1C), 128.4 (2C), 130.9 (1C), 131.4 (1C), 135.1 (1C), 139.8 (1C), 158.7 (1C), 164.2 (1C), 170.9 (1C); HR-ESI-MS [M + H]$^+$ calculated for $C_{23}H_{16}F_4N_2O$, 412.1199, found

412.3796; anal. calcd for $C_{23}H_{16}F_4N_2O$ (412.12) C, 66.99; H, 3.91; F, 18.43; N, 6.79; O, 3.88; found: C, 67.01; H, 3.90; N, 6.77.

**3.4.23. 2-(1-(2-Fluoro-[1,1′-biphenyl]-4-yl)ethyl)-5-(4-(methylthio)phenyl)-1,3,4-oxadiazole (27).** White amorphous solid; yield: 78%; $^1$H-NMR (400 MHz, $CDCl_3$; $\delta$, ppm): 1.42 (d, $J$ = 7.1 Hz, 3H), 2.01 (s, 3H), 3.52 (q, $J$ = 7.1 Hz, 1H), 7.25–7.28 (m, 5H), 7.29 (d, $J$ = 7.8 Hz, 2H), 7.49–7.51 (m, 3H), 7.86 (d, $J$ = 7.8 Hz, 2H); $^{13}$C-NMR (150 MHz, DMSO-$d_6$) $\delta$ 16.2 (1C), 20.3 (1C), 41.1 (1C), 116.4 (1C), 121.8 (1C), 125.0 (2C), 126.8 (1C), 127.6 (5C), 128.2 (1C), 128.8 (2C), 131.9 (1C), 136.1 (1C), 140.2 (1C), 143.3 (1C), 160.7 (1C), 164.2 (1C), 172.3 (1C); HR-ESI-MS $[M + H]^+$ calculated for $C_{23}H_{19}FN_2OS$, 390.1202, found 390.4732; anal. calcd for $C_{23}H_{19}FN_2OS$ (390.12) C, 70.75; H, 4.90; F, 4.87; N, 7.17; O, 4.10; S, 8.21; found: C, 70.76; H, 4.91; N, 7.14.

**3.4.24. 2-Bromo-4-(5-(1-(2-fluoro-[1,1′-biphenyl]-4-yl)ethyl)-1,3,4-oxadiazol-2-yl)phenol (28).** Brownish amorphous solid; yield: 75%; $^1$H-NMR (400 MHz, $CDCl_3$; $\delta$, ppm): 1.33 (d, $J$ = 6.8 Hz, 3H), 3.42 (q, $J$ = 6.8 Hz, 1H), 7.23–7.25 (m, 5H), 7.29 (d, $J$ = 7.0 Hz, 1H), 7.32 (d, $J$ = 7.0 Hz, 1H), 7.89–7.91 (m, 3H), 8.22 (d, $J$ = 1.2 Hz, 1H), 10.55 (br.s, 1H); $^{13}$C-NMR (150 MHz, DMSO-$d_6$) $\delta$ 19.3 (1C), 40.7 (1C), 109.7 (1C), 115.4 (1C), 116.9 (1C), 126.0 (1C), 127.2 (1C), 127.6 (3C), 128.2 (1C), 128.4 (2C), 129.0 (1C), 130.9 (1C), 131.0 (1C), 135.5 (1C), 139.2 (1C), 152.3 (1C), 159.7 (1C), 163.2 (1C), 171.3 (1C); HR-ESI-MS $[M + H]^+$ calculated for $C_{22}H_{16}BrFN_2O_2$, 438.9535, found 439.1737; anal. calcd for $C_{22}H_{16}BrFN_2O_2$ (438.95) C, 60.15; H, 3.67; Br, 18.19; F, 4.32; N, 6.38; O, 7.28; found: C, 60.16; H, 3.65; N, 6.39.

**3.4.25. 2-(2-Fluoro-[1,1′-biphenyl]-4-yl)-5-(1-(2-fluoro-[1,1′-biphenyl]-4-yl)ethyl)-1,3,4-oxadiazole (29).** Brown amorphous solid; yield: 72%; $^1$H-NMR (400 MHz, $CDCl_3$; $\delta$, ppm): 1.25 (d, $J$ = 7.0 Hz, 3H), 3.06 (q, $J$ = 7.0 Hz, 1H), 7.47–7.53 (m, 8H), 7.59–7.88 (m, 5H), 7.78 (d, $J$ = 7.5 Hz, 1H), 7.87 (d, $J$ = 7.5 Hz, 1H), 8.31 (s, 1H); $^{13}$C-NMR (150 MHz, DMSO-$d_6$) $\delta$ 19.7 (1C), 41.7 (1C), 116.4 (1C), 124.7 (1C), 126.2 (1C), 126.8 (1C), 127.2 (1C), 127.4 (1C), 127.8 (7C), 128.7 (4C), 129.9 (1C), 131.9 (1C), 133.1 (1C), 136.5 (1C), 139.3 (2C), 159.5 (1C), 164.2 (1C), 172.3 (1C); HR-ESI-MS $[M + H]^+$ calculated for $C_{28}H_{20}F_2N_2O$, 438.1649, found 438.4940; anal. calcd for $C_{28}H_{20}F_2N_2O$ (438.16) C, 76.70; H, 4.60; F, 8.67; N, 6.39; O, 3.65; found: C, 76.73; H, 4.57; N, 6.40.

**3.4.26. 2-(1-(2-Fluoro-[1,1′-biphenyl]-4-yl)ethyl)-5-(5-methylthiophen-2-yl)-1,3,4-oxadiazole (30).** White amorphous solid; yield: 82%; $^1$H-NMR (400 MHz, $CDCl_3$; $\delta$, ppm): 1.31 (d, $J$ = 7.1 Hz, 3H), 2.41 (s, 3H), 3.41 (q, $J$ = 7.1 Hz, 1H), 6.88–6.90 (m, 6H), 7.13 (d, $J$ = 7.6 Hz, 1H), 7.56–7.60 (m, 3H); $^{13}$C-NMR (150 MHz, DMSO-$d_6$) $\delta$ 16.4 (1C), 20.3 (1C), 41.7 (1C), 113.4 (1C), 124.7 (1C), 127.2 (1C), 127.4 (1C), 127.8 (3C), 128.2 (1C), 128.4 (2C), 130.9 (1C), 133.1 (1C), 136.5 (1C), 141.2 (1C), 142.5 (1C), 160.7 (1C), 162.2 (1C), 173.3 (1C); HR-ESI-MS $[M + H]^+$ calculated for $C_{21}H_{17}FN_2OS$, 364.1046, found 364.4359; anal. calcd for $C_{21}H_{17}FN_2OS$ (364.10) C, 69.21; H, 4.70; F, 5.21; N, 7.69; O, 4.39; S, 8.80; found: C, 69.22; H, 4.73; N, 7.67.

**3.4.27. 3-(5-(1-(2-Fluoro-[1,1′-biphenyl]-4-yl)ethyl)-1,3,4-oxadiazol-2-yl)benzene-1,2-diol (31).** Off white amorphous solid; yield: 92%; $^1$H-NMR (400 MHz, $CDCl_3$; $\delta$, ppm): 1.25 (d, $J$ = 6.4 Hz, 3H), 3.42 (q, $J$ = 6.4 Hz, 1H), 6.87 (d, $J$ = 7.0 Hz, 1H), 7.16–7.20 (m, 5H), 7.25 (t, $J$ = 7.1 Hz, 1H), 7.37 (d, $J$ = 7.1 Hz, 1H), 7.81–7.84 (m, 3H), 10.52 (br.s, 2H); $^{13}$C-NMR (150 MHz, DMSO-$d_6$) $\delta$ 18.9 (1C), 41.1 (1C), 108.5 (1C), 113.1 (1C), 115.4 (1C), 125.9 (1C), 127.0 (1C), 127.4 (3C), 128.2 (1C), 128.8 (2C), 129.8 (1C), 131.9 (1C), 136.3 (1C), 140.2 (1C), 146.6 (1C), 148.9 (1C), 160.7 (1C), 165.2 (1C), 173.5 (1C); HR-ESI-MS $[M + H]^+$ calculated for $C_{22}H_{17}FN_2O_3$, 376.1223, found 376.3804; anal. calcd for $C_{22}H_{17}FN_2O_3$ (376.12) C, 70.20; H, 4.55; F, 5.05; N, 7.44; O, 12.75; found: C, 70.22; H, 4.53; N, 7.46.

**3.4.28. 2-(1-(2-Fluoro-[1,1′-biphenyl]-4-yl)ethyl)-5-(2-nitrophenyl)-1,3,4-oxadiazole (32).** White amorphous solid; yield: 83%; $^1$H-NMR (400 MHz, $CDCl_3$; $\delta$, ppm): 1.31 (d, $J$ = 6.4 Hz, 3H), 2.69 (q, $J$ = 6.4 Hz, 1H), 7.46–7.51 (m, 3H), 7.53–7.65 (m, 2H), 7.82–7.86 (m, 3H), 8.02 (d, $J$ = 8.2 Hz, 2H), 8.14 (d, $J$ = 8.6 Hz, 1H), 8.59 (s, 1H); $^{13}$C-NMR (150 MHz, DMSO-$d_6$) $\delta$ 19.3 (1C), 42.7 (1C), 107.4 (1C), 116.4 (1C), 119.7 (1C), 126.2 (1C), 127.3 (3C), 128.1 (2C), 128.5 (3C), 129.3 (1C), 130.9 (1C), 136.5 (1C), 138.2 (1C), 139.7 (1C), 158.7 (1C), 163.0 (1C), 172.3 (1C); HR-ESI-MS $[M + H]^+$ calculated for $C_{22}H_{16}FN_3O_3$, 389.1176, found 389.3791; anal. calcd for $C_{22}H_{16}FN_3O_3$ (389.12) C, 67.86; H, 4.14; F, 4.88; N, 10.79; O, 12.33; found: C, 67.85; H, 4.16; N, 4.90.

## 4. Conclusion

Twenty-eight novel oxadiazole derivatives (**5–32**) based on the commercially available drug (*S*)-flurbiprofen have been synthesized in very good yields through multistep reactions. The synthesized analogues were confirmed by way of HR-MS ($ESI^+$), and $^1$H-NMR spectroscopic procedures. As a final point, the compounds were tested for their *in vitro* urease inhibitory activity. All the compounds showed varying degrees of inhibition activity. Fourteen compounds **20**, **26**, **30**, **24**, **21**, **16**, **28**, **31**, **32**, **7**, **19**, **13**, **10**, and **6** were found as the supreme powerful urease inhibitors having $IC_{50}$ values of 12 ± 0.9 to 20 ± 0.5 μM, better than the standard thiourea ($IC_{50}$ = 22 ± 2.2 μM). On the other hand, nine compounds exhibited significant activity, while five compounds showed moderate to less urease inhibitory activity. The docking results indicated that compounds **20**, **26**, **30**, **24**, **21**, **16**, **28**, **31**, **32**, **7**, **19**, **13**, **10**, and **6** had lower docking scores than the reference compound and revealed better interactions with the urease enzyme, which was in agreement with the experimental study.

## Author contributions

S. A. and A. S. synthesized the compounds. A. A. and M. K. wrote the original draft of the manuscript. A. W. and A. K. conducted activity and docking study. A. F. A. and M. A. performed structural elucidation. M. K. and A. Al supervised the project and assisted in reviewing and editing the manuscript. All authors have read and agreed to the published version of the manuscript.

## Conflicts of interest

The authors declare no conflict of interest.

## Acknowledgements

Authors are thankful to researchers supporting project number (RSP2023R335), King Saud University, Riyadh, Saudi Arabia.

## References

1 K. Biernacki, M. Daśko, O. Ciupak, K. Kubiński, J. Rachon and S. Demkowicz, Novel 1,2,4-oxadiazole derivatives in drug discovery, *Pharmaceuticals*, 2020, **13**(6), 111.

2 I. O. Alisi, A. Uzairu and S. E. Abechi, Free radical scavenging mechanism of 1,3,4-oxadiazole derivatives: thermodynamics of O–H and N–H bond cleavage, *Heliyon*, 2020, **6**(3), e03683.

3 A. S. Alp, G. Kilcigil, E. D. Özdamar, T. Çoban and B. Eke, Synthesis and evaluation of antioxidant activities of novel 1,3,4-oxadiazole and imine containing 1*H*-benzimidazoles, *Turk. J. Chem.*, 2015, **39**(1), 42–53.

4 M. M. G. El-Din, M. I. El-Gamal, M. S. Abdel-Maksoud, K. H. Yoo and C.-H. Oh, Synthesis and *in vitro* antiproliferative activity of new 1,3,4-oxadiazole derivatives possessing sulfonamide moiety, *Eur. J. Med. Chem.*, 2015, **90**, 45–52.

5 B. B. Kashid, P. H. Salunkhe, B. B. Dongare, K. R. More, V. M. Khedkar and A. A. Ghanwat, Synthesis of novel of 2, 5-disubstituted 1,3,4-oxadiazole derivatives and their *in vitro* anti-inflammatory, anti-oxidant evaluation, and molecular docking study, *Bioorg. Med. Chem. Lett.*, 2020, **30**(12), 127136.

6 M. Khan, A. Alam, K. M. Khan, U. Salar, S. Chigurupati, A. Wadood, F. Ali, J. I. Mohammad, M. Riaz and S. Perveen, Flurbiprofen derivatives as novel α-amylase inhibitors: Biology-oriented drug synthesis (BIODS), *in vitro*, and *in silico* evaluation, *Bioorg. Chem.*, 2018, **81**, 157–167.

7 S. Shah, M. Khan, M. Ali, A. Wadood, A. Ur Rehman, Z. Shah, M. Yousaf, U. Salar and K. M. Khan, Bis-1,3,4-Oxadiazole Derivatives as Novel and Potential Urease Inhibitors; Synthesis, *In Vitro*, and *In Silico* Studies, *Med. Chem.*, 2022, **18**(7), 820–830.

8 A. R. Nesaragi, R. R. Kamble, S. Dixit, B. Kodasi, S. R. Hoolageri, P. K. Bayannavar, J. P. Dasappa, S. Vootla, S. D. Joshi and V. M. Kumbar, Green synthesis of therapeutically active 1,3,4-oxadiazoles as antioxidants, selective COX-2 inhibitors and their *in silico* studies, *Bioorg. Med. Chem. Lett.*, 2021, **43**, 128112.

9 S. G. Musharraf, A. Bibi, N. Shahid, M. Najam-ul-Haq, N. Ambreen, M. Khan, K. M. Khan and M. I. Choudhary, Benzimidazole, coumrindione and flavone derivatives as alternate UV laser desorption ionization (LDI) matrices for peptides analysis, *Chem. Cent. J.*, 2013, **7**(1), 1–13.

10 K. Mohammed Khan, M. Khan, N. Ambreen, F. Rahim, S. Naureen, S. Perveen, M. Iqbal Choudhary and W. Voelter, Synthesis and β-glucuronidase inhibitory potential of benzimidazole derivatives, *Med. Chem.*, 2012, **8**(3), 421–427.

11 A. Alam, M. Ali, N. U. Rehman, S. Ullah, S. A. Halim, A. Latif, Zainab, A. Khan, O. Ullah and S. Ahmad, Bio-oriented synthesis of novel (*S*)-flurbiprofen clubbed hydrazone Schiff's bases for diabetic management: *In vitro* and *in silico* studies, *Pharmaceuticals*, 2022, **15**(6), 672.

12 S. Ahmad, M. Khan, M. I. A. Shah, M. Ali, A. Alam, M. Riaz and K. M. Khan, Synthetic Transformation of 2-{2-Fluoro [1,1′-biphenyl]-4-yl} Propanoic Acid into Hydrazide–Hydrazone Derivatives: *In Vitro* Urease Inhibition and *In Silico* Study, *ACS Omega*, 2022, **7**(49), 45077–45087.

13 P. Çıkla, E. Tatar, İ. Küçükgüzel, F. Şahin, D. Yurdakul, A. Basu, R. Krishnan, D. B. Nichols, N. Kaushik-Basu and Ş. G. Küçükgüzel, Synthesis and characterization of flurbiprofen hydrazide derivatives as potential anti-HCV, anticancer and antimicrobial agents, *Med. Chem. Res.*, 2013, **22**, 5685–5699.

14 A. Khullar, A review on Flurbiprofen: Therapeutic challenges in Emerging Active Metabolizing Biphenyl, *Bull. Pure Appl. Sci.*, 2020, **39**, 77–89.

15 P. Çıkla, E. Tatar, İ. Küçükgüzel, *et al.*, Synthesis and characterization of flurbiprofen hydrazide derivatives as potential anti-HCV, anticancer and antimicrobial agents, *Med. Chem. Res.*, 2013, **22**, 5685–5699.

16 S. Aydin, N. Kaushik-Basu, P. Arora, B. Amartya, D. Nichols, T. T TALELE, M. Akkurt, İ. Çelik, O. Büyükgüngör and Ş. G. Küçükgüzel, Microwave assisted synthesis of some novel Flurbiprofen hydrazidehydrazones as anti-HCV NS5B and anticancer agents, *Marmara Pharm. J.*, 2013, **17**(1), 26–34.

17 K. A. Musa and L. A. Eriksson, Photochemical and photophysical properties, and photodegradation mechanism, of the non-steroid anti-inflammatory drug Flurbiprofen, *J. Photochem. Photobiol., A*, 2009, **202**(1), 48–56.

18 S. Sagdinc and H. Pir, Spectroscopic and DFT studies of flurbiprofen as dimer and its Cu (II) and Hg (II) complexes, *Spectrochim. Acta, Part A*, 2009, **73**(1), 181–194.

19 M. Taha, N. H. Ismail, S. Imran, A. Wadood, M. Ali, F. Rahim, A. A. Khan and M. Riaz, Novel thiosemicarbazide–oxadiazole hybrids as unprecedented inhibitors of yeast α-glucosidase and *in silico* binding analysis, *RSC Adv.*, 2016, **6**(40), 33733–33742.

20 M. Taha, T. Noreen, S. Imran, F. Nawaz, S. Chigurupati, M. Selvaraj, F. Rahim, N. Hadiani Ismail, A. Kumar and A. Mosaddik, Synthesis, α-amylase inhibition and molecular docking study of bisindolylmethane sulfonamide derivatives, *Med. Chem. Res.*, 2019, **28**, 2010–2022.

21 F. Rahim, H. Ullah, M. T. Javid, A. Wadood, M. Taha, M. Ashraf, A. Shaukat, M. Junaid, S. Hussain and W. Rehman, Synthesis, *in vitro* evaluation and molecular docking studies of thiazole derivatives as new inhibitors of α-glucosidase, *Bioorg. Chem.*, 2015, **62**, 15–21.

22 M. Taha, N. H. Ismail, S. Imran, A. Wadood, F. Rahim, S. M. Saad, K. M. Khan and A. Nasir, Synthesis, molecular docking and α-glucosidase inhibition of 5-aryl-2-(6′-nitrobenzofuran-2′-yl)-1,3,4-oxadiazoles, *Bioorg. Chem.*, 2016, **66**, 117–123.

23 M. Nawaz, M. Taha, F. Qureshi, N. Ullah, M. Selvaraj, S. Shahzad, S. Chigurupati, S. A. Abubshait, T. Ahmad and

S. Chinnam, Synthesis, α-amylase and α-glucosidase inhibition and molecular docking studies of indazole derivatives, *J. Biomol. Struct. Dyn.*, 2022, **40**(21), 10730–10740.

24 W. Yu, G. Huang, Y. Zhang, H. Liu, L. Dong, X. Yu, Y. Li and J. Chang, I2-mediated oxidative C–O bond formation for the synthesis of 1,3,4-oxadiazoles from aldehydes and hydrazides, *J. Org. Chem.*, 2013, **78**(20), 10337–10343.

25 W.-J. Mao, P.-C. Lv, L. Shi, H.-Q. Li and H.-L. Zhu, Synthesis, molecular docking and biological evaluation of metronidazole derivatives as potent Helicobacter pylori urease inhibitors, *Bioorg. Med. Chem.*, 2009, **17**(21), 7531–7536.

26 G. Akyüz, Synthesis and urease inhibition studies of some new quinazolinones, *J. Heterocycl. Chem.*, 2021, **58**(5), 1164–1170.

27 Z. Amtul, R. Siddiqui and M. Choudhary, Chemistry and mechanism of urease inhibition, *Curr. Med. Chem.*, 2002, **9**(14), 1323–1348.

28 L. Mazzei, U. Contaldo, F. Musiani, M. Cianci, G. Bagnolini, M. Roberti and S. Ciurli, Inhibition of Urease, a Ni-Enzyme: The Reactivity of a Key Thiol With Mono-and Di-Substituted Catechols Elucidated by Kinetic, Structural, and Theoretical Studies, *Angew. Chem.*, 2021, **133**(11), 6094–6100.

29 A. Wadood, A. Ajmal, M. Junaid, A. U. Rehman, R. Uddin, S. S. Azam, A. Z. Khan and A. Ali, Machine Learning-based Virtual Screening for STAT3 Anticancer Drug Target, *Curr. Pharm. Des.*, 2022, **28**(36), 3023–3032.

30 B. Bano, K. M. Khan, B. Fatima, M. Taha, N. H. Ismail, A. Wadood, M. Ghufran and S. Perveen, Synthesis, *in vitro* β-glucuronidase inhibitory potential and molecular docking studies of quinolines, *Eur. J. Med. Chem.*, 2017, **139**, 849–864.